Air Charge Control for Turbocharged Spark Ignition Engines with Internal Exhaust Gas Recirculation

Donghoon Lee, Li Jiang, Hakan Yilmaz and Anna G. Stefanopoulou

***Abstract*— This paper presents the design of transient cylinder charge control, based on a cycle-averaged mean-value model for a turbocharged spark ignition direct injection engine equipped with intake and exhaust variable camshafts. The control-oriented model, parameterized using dynamometer measurements, has demonstrated its capability of capturing engine static and dynamic behavior of throttled conditions. The transient effects of throttling and variable valve timing on the cylinder charge over part-load and lightly boosted conditions are first analyzed to investigate the dynamic interactions between the electronic throttle and the valve overlap through variable camshafts. Given the much faster dynamics of an electronic throttle, a nonlinear feedforward and feedback throttle compensator, in reference to its static set-points, is employed here to improve the transient response of cylinder charge. It has been shown in simulation results that the combined use of both compensators can considerably improve transient engine performance.**

I. Introduction

We present in this paper an effort to minimize the detrimental effects of high levels of exhaust gas recirculation (EGR) in the drivability of a turbocharged Spark Ignition Direct Injection (SIDI) engine equipped with dual cam phasing capability, as shown in Fig. 1. In such an engine

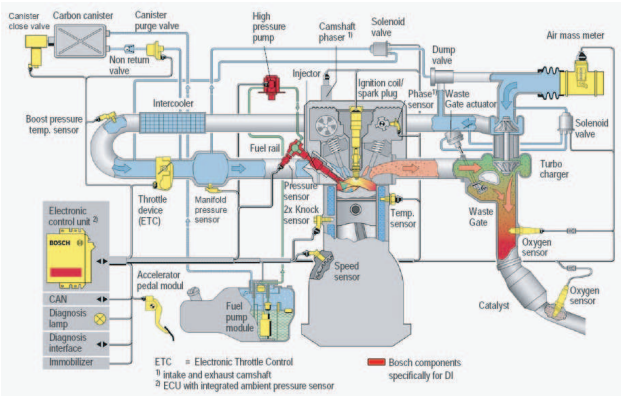

Fig. 1. Configuration of a turbocharged gasoline direct injection engine equipped with variable intake and exhaust camshafts

platform, the throttle, the turbocharger wastegate, and the Variable Valve Timing (VVT) system are three actuators in the air path system for the control of cylinder charge. The VVT system with variable camshafts allows flexible valve overlap, hence, enables high level of internal EGR (iEGR), which, if there is no combustion stability problem, typically reduces fuel and NOx emissions.The benefits of the high level of iEGR for fuel consumption come with well known problems associated with drivability [1], [2] or control of transient air charge. In order to ensure accurate and fast delivery of the demanded air charge, appropriate control and coordination of the three actuators are required to realized the benefits of these advanced automotive technologies. Therefore, various Computer Aided Control System Design (CACSD) methods, relying on control-oriented models, have been applied to solve this problem. Literature that addresses the control of variable camshafts for the control of transient torque response, such as [1] for a system with mechanical throttle and [2] for one with electronic throttle, provides great insight into the coordination of the throttle and the VVT system. However, the coordinated control of these three actuators in the air path system has not been investigated for a turbocharged engine. Applicable models of turbocharged gasoline engines can be found in [3], [4], [5], [6]. Literature that addresses the control of wastegate in gasoline applications, such as [7], [8] for a system with mechanical throttle and [5] for one with electronic throttle, provides valuable insight into the coordination of the throttle and the turbocharger wastegate. In parallel with the air-path control loop, Air-to-Fuel Ratio (AFR) is regulated in the fuel path using feedback information from an Exhaust Gas Oxygen (EGO) sensor. Even though AFR regulation is not discussed in this paper, the closed-loop control of fuel injection can be aided by the indirect air-charge estimation approach developed here. Details of air charge estimation via an exhaust manifold pressure observer are discussed in [9] and [10]. However, the effects of the VVT system and the associated internal gas recirculation have not been explicitly studied by Buckland *et al.*

The selection of a performance variable is not as straightforward because one has to take into account its ability to represent the overall performance objectives (e.g., efficiency, emissions, drivability) and its ability to correlate with the available measurements. This paper focus on improving the transient response of cylinder charge flow rate during tip-ins via the use of two compensators added on the base throttle signal. The first compensator, called valve compensator, minimizes the deleterious effects of valve overlap changes on cylinder air flow. The second compensator, called pressure compensator, modifies the base throttle signal by best utilizing the available boost pressure. Therefore, the work

This work is funded by U.S. Department of Energy and Robert Bosch LLC.

D. Lee (huni@umich.edu) and A.G. Stefanopoulou (annastef@umich.edu) are with Mechanical Engineering Department in the University of Michigan, Ann Arbor. L. Jiang (li.jiang@us.bosch.com) and H. Yilmaz (hakan.yilmaz@us.bosch.com) are with Robert Bosch LLC, Farmington Hills.

presented here can be applied over part-load and lightly boost operation conditions when the wastegate remains passive[1]. A control-oriented model for the target engine system is first developed and parameterized with dynamometer measurements collected over a wide range of operation conditions and various gasoline-ethanol fuel blends. Developed based on the model in [6], the engine model consists of a mean value model to simulate the cycle-average behavior of the air-path system and a discrete event model to capture the particular behavior during each stroke (i.e., intake, compression, combustion/expansion, exhaust). As presented in Section II, the parameterized engine model is able to predict the dynamic engine behavior with gasoline and ethanol fuels up to E85 (85% ethanol and 15% gasoline in volume). The static VVT scheduling scheme that take various engine performance variables (e.g., efficiency, emission, combustion stability) into consideration is described in Section III. In Section IV, the dynamic interaction between the throttle and the valve overlap and their transient effects on the intake manifold pressure and cylinder charge is analyzed. Then, the valve compensator is designed to improve the transient behaviors of cylinder charge during tip-ins when the VVT system transits from one set-point position to other as commanded by the static VVT schedule. To further improve the transient response of cylinder charge over high-load conditions, a pressure throttle compensator is introduced in Section V. As shown in the simulation results, the combined use of the feedforward and feedback throttle compensate can significantly improve the transient cylinder charge response. Finally, summary of the current work and future work are discussed in Section VI.

II. Control-Oriented Model and Validation

This work develops a model on the basis of the one presented in [6] that follows the principles of mass and energy conservation and the Newton's law for turbocharger dynamics. The schematic in Fig. 2 shows the 7 states, namely, two states for the boost pressure p_b and temperature T_b; two states for the intake manifold pressure p_{im} and temperature T_{im}; two states for the exhaust manifold mass p_{ex} and temperature T_{ex}; one state for the turbocharger connecting shaft rotational speed N_{tc}. In this section, only the modifications from the original model in [6] are discussed, which are the modeling of cylinder charge flow rate (also known as engine pumping rate) and the state reduction of exhaust manifold temperature following an isothermal assumption. For details of the model, please refer to [6].

Based on dynamometer measurements, the mass air flow rate into the cylinder W_{cyl} can be modeled as a function of intake manifold pressure p_{im}, engine speed N, and intake and exhaust valve overlap v

$$W_{cyl} = F(p_{im}, N, v) = \alpha_1(N, v)p_{im} + \alpha_2(N, v), \qquad (1)$$

[1]The duty cycle of the turbocharger wastegate is set to zero so that its opening is govern by the spring force, exhaust gas back-pressure, and boost pressure.

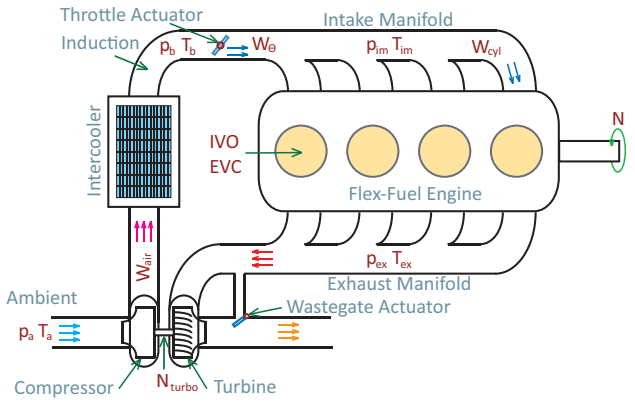

Fig. 2. Schematic of turbocharged spark ignition direct injection engine equipped with variable intake and exhaust camshafts.

where α_1 and α_2 are polynomials in N and v. Fig. 3 shows that W_{cyl} can be modeled as a liner function of p_{im} while α_1 and α_2 depend on N and v. It should be noted that the behavior of the VVT system in this turbocharged engine is more complex than what has been observed and documented in the Naturally Aspirated (NA) Spark Ignition (SI) engine. As shown in Fig. 3, when the intake manifold pressure is lower than the atmosphere pressure (i.e., $p_{im} < 1\ bar$), an increased valve overlap decreases the fresh charge flow rate in the cylinders, which has been observed in the conventional NA SI engine. However, when the intake manifold pressure is higher than the atmosphere pressure (i.e., $p_{im} > 1\ bar$), an increased valve overlap increases the cylinder charge flow rate.

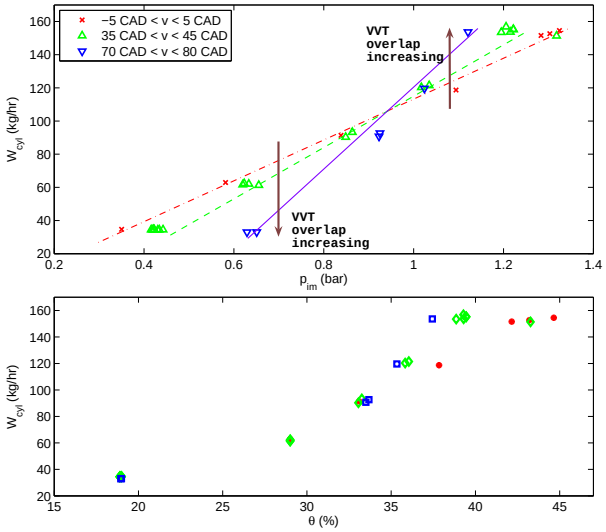

Fig. 3. Cylinder pumping flow W_{cyl} versus intake manifold pressure p_{im} with various intake and exhaust valve overlaps v at N = 2000 RPM.

Simulation results have suggested that the isothermal assumption is acceptable for the modeling of exhaust manifold dynamics

$$\frac{dp_{ex}}{dt} = \frac{RT_{ex}}{V_{ex}}(W_{in} - W_{out}), \qquad (2)$$

where R and V_{ex} denote the ideal gas constant and the exhaust manifold volume, respectively. $T_{ex} = T_{bd}$ is the blowdown temperature which is modeled based on an ideal isochoric combustion of the injected fuel followed by an isotropic expansion. The heat generated during combustion depends on the low heating value and quantity of the injected fuel [6].

The model has been parameterized using steady-state dynamometer measurements for gasoline fuel from 800 RPM up to 4500 RPM with various control set-points for throttle angle, wastegate duty cycle, fuel injection and spark angle, positions of Intake Valve Open (IVO) and Exhaust Valve Closing (EVC), and fuel rail pressure. The parameterized mean-value model captures the transients with reasonable accuracy for both fuels: gasoline (E0) and fuel with 85% volumetric ethanol content (E85). Validation of the transient behavior during a step change in the throttle angle is shown in Fig. 4 and 5 for E0 and E85, respectively.

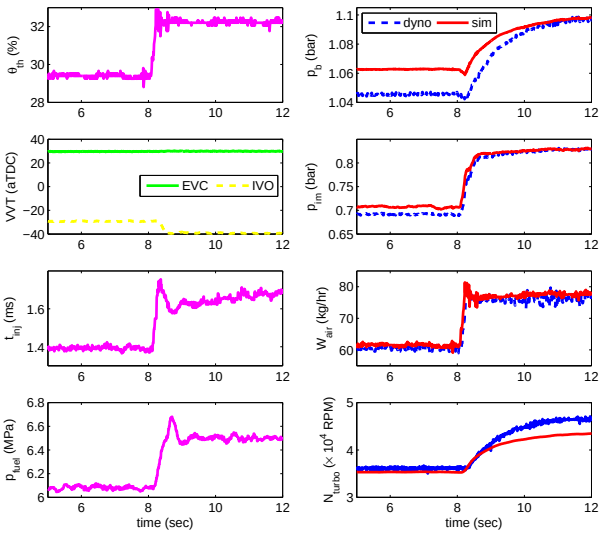

Fig. 4. Comparison between dynamometer measurement and model simulation for throttle step change with E0 fuel and a fixed wastegate duty cycle at 0% at N = 2000 RPM; dynamometer engine inputs are presented in the first column and corresponding engine outputs (blue dashed lines) are compared with simulation results (red solid lines) in the second column.

Subplots of the first column in Fig. 4 and 5 show the engine model inputs, and those of the second column allow a direct comparison between the predicted (red solid lines) and measured engine outputs (blue dashed lines). At 2000 RPM for E0 both the measured and predicted outputs show undershoots in the boost pressure, p_b, and overshoot in the air flow rate through the compressor, W_{air}. As shown in in Fig. 5, the model also captures the undershoot in boost pressure, p_b, caused by a throttle angle change at 2500 RPM for E85.

III. Static Schedule of VVT

In this section, a static schedule for the intake and exhaust valve overlap is proposed to achieve maximum iEGR at medium load, stable combustion at low load, and maximum

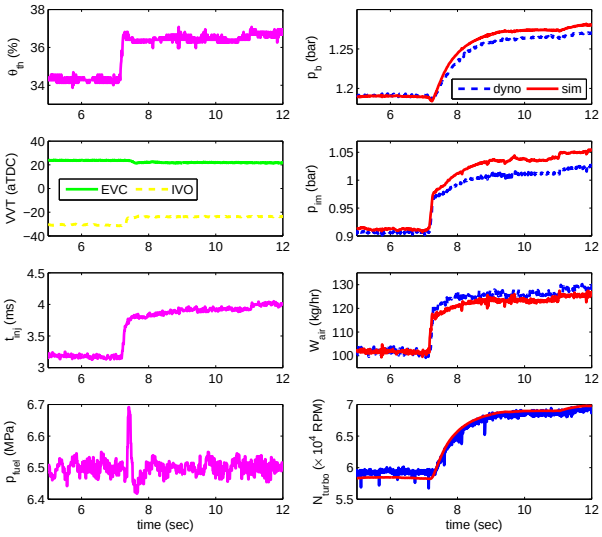

Fig. 5. Comparison between dynamometer measurement and model simulation for throttle step change with E85 fuel and a fixed wastegate duty cycle at 0% at N = 2500 RPM; dynamometer engine inputs are presented in the first column and corresponding engine outputs (blue dashed lines) are compared with simulation results (red solid lines) in the second column.

torque at high load [1]. Since the electronic throttle is the actuator that has the most control authority over cylinder charge at part-load and lightly-boosted conditions, the static valve overlap is scheduled with respect to the throttle angle.

In Fig. 6, the plots of the first and second row show the steady-state cylinder charge flow rate, W_{cyl}, and intake manifold pressure, p_{im}, with respect to the throttle angle, θ, at three valve overlap values(i.e., v = 0, 40, 80 CAD). The cylinder charge flow rate at different valve overlap values are approximately same at low load with $\theta < 20\%$. At medium load with $20\% < \theta \leq 40\%$, the cylinder charge flow rate decreases with an increased valve overlap. At high load with $\theta > 40\%$, however, the cylinder charge flow rate increases with an increased valve overlap at a given throttle angle.

It is important to note that at low throttle valves, during small downstream-to-upstream pressure ratio p_{im}/p_b, when flow through the throttle body occurs at sonic conditions, overlap does not affect the steady-state cylinder air flow but it has detrimental effect as can be seen in Fig. 7. This zero DC gain, yet strong transient influence of the overlap on flow arises from the inlet manifold filling dynamics with p_{im} adjusting to higher values as overlap increases as shown in Fig. 6 (second subplot).

Two overlap scheduling schemes, denoted as v_{egr} and v_{air}, are shown in the third subplot in Fig. 6. One scheduling scheme for v_{egr} is derived to achieve maximum iEGR level subject to stable combustion at low load and maximum torque at high load; 1) near idle engine conditions ($\theta <$ 20%), VVT overlap is scheduled to be zero for idle combustion stability 2) at high loads ($\theta \geq 40\%$) near WOT, the overlap is set to be 80 CAD such that W_{cyl} can be maximized, and 3) for part loads, overlap is selected to achieve the maximum iEGR with a smooth transition between v = 0

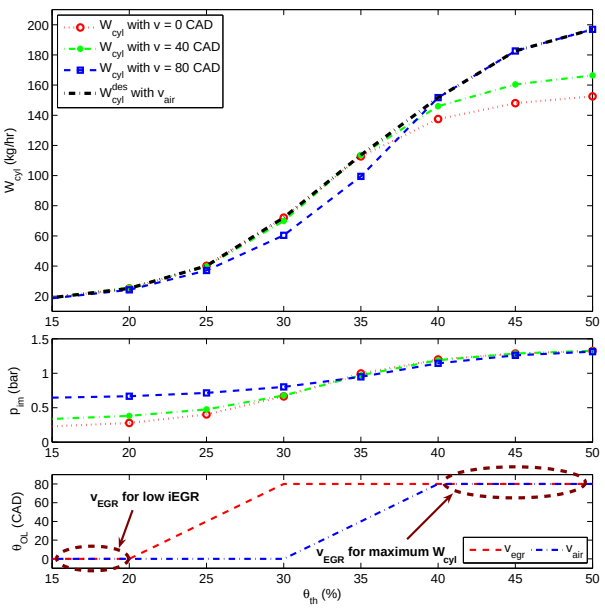

Fig. 6. Cylinder pumping flow rate W_{cyl} and intake manifold pressure p_{im} with respect to throttle angles θ for various intake and exhaust valve overlaps v and corresponding VVT overlap scheduling scheme v at N = 2000 RPM.

CAD and v = 80 CAD at the throttle range of 20% $\leq \theta <$ 40%. Apart from v_{egr}, a reference valve overlap defined as v_{air} in Fig. 6 is determined to maximize cylinder air flow rate given throttle angle. This desired maximum cylinder flow rate W_{cyl}^{des} (black dashed line) is presented in the first plot in Fig. 6. Based on the two different overlap scheme, v_{egr} and v_{air}, a model-based throttle compensator that reduces the deleterious effect of overlap changes on cylinder air flow will be discussed in the next section.

IV. Valve Compensator Design

A valve compensator with an electronic throttle for a NA throttled engine is designed in [2] to remove or reduce the effect of the VVT transients on the cylinder charged, in which employs θ_{th}^{*} is employed as a virtual actuator. The effects of step changes in valve overlap on the cylinder charge flow rate at throttle angles of 20% and 40% are simulated and illustrated in Fig. 7. The valve overlap increase at lightly boosted conditions when $p_{im} > 1$ *bar* and $\theta_{th} = 40\%$ leads to the transition to an increased steady-state cylinder charge flow rate, as observed in Fig. 3. The same step change in valve overlap at part load conditions when $p_{im} < 1$ *bar* and $\theta_{th} = 20\%$, however, leads to the transitions with large overshoots and undershoots with no steady-state cylinder flow rate change. The valve compensator design, presented in [2] for a NA engine, is modified here to compensate for these deleterious valve overlap transients.

The compensator design also takes into account the fact that the boost pressure, p_b, varies at different engine speeds and loads in a turbocharged engine. Here, the intake manifold pressure p_{im}, boost pressure p_b, engine speed N, and overlap v are considered available from measurements. Moreover,

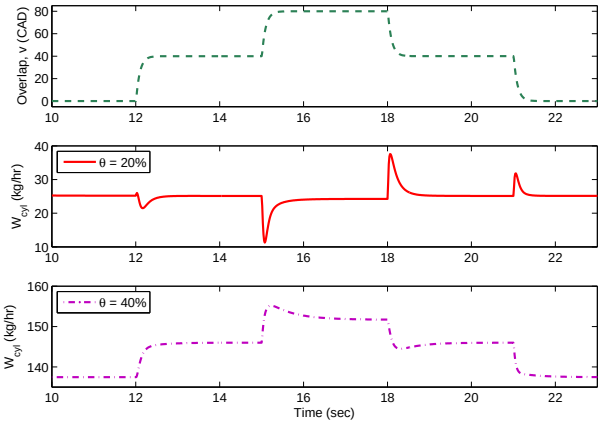

Fig. 7. Cylinder air charge rate W_{cyl} response of the turbocharged engine on VVT overlap v step changes; engine speed is 2000 RPM and throttle is fixed at θ = 20% (second plot) and θ = 40% (third plot).

to further simplify the engine model for the compensator design, the intake manifold is assumed to be isothermal so that the state of intake manifold temperature, T_{im}, can be eliminated.

$$\dot{p}_{im} = K_{im}\left(W_{\theta} - W_{cyl}\right), \tag{3}$$

such that first order dynamics can be used for the compensator design with the throttle air flow determined by

$$W_{\theta} = g_1(\theta, p_b) g_2(p_{im}/p_b), \tag{4}$$

where $g_1 = A_e(\theta)\dfrac{p_b}{\sqrt{RT_{im}}}$

$$g_2 = \begin{cases} \sqrt{\dfrac{\gamma}{\gamma+1}}\left(\dfrac{2}{\gamma+1}\right)^{\frac{1}{\gamma-1}} & \text{if } \dfrac{p_{im}}{p_b} \leq r_c \\ \sqrt{\dfrac{\gamma}{\gamma-1}\left(\left(\dfrac{p_{im}}{p_b}\right)^{\frac{2}{\gamma}} - \left(\dfrac{p_{im}}{p_b}\right)^{\frac{\gamma+1}{\gamma}}\right)} & \text{if } \dfrac{p_{im}}{p_b} > r_c \end{cases}$$

with $K_{im} = RT_{im}/V_{im}$, and T_{im} and V_{im} correspond to the intake manifold pressure and volume, respectively, $A_e(\theta)$ indicates effective cross section area and $r_c = (2/(\gamma+1))^{\gamma/(\gamma-1)}$ denotes critical compression ratio, which draws a distinction between sonic and subsonic flows. Additionally, the VVT actuator mechanism dynamics are modeled by

$$\dot{v}_{egr}^{act} = -\frac{1}{\tau_{VVT}}\left(v_{egr} - v_{egr}^{act}\right), \quad \tau_{VVT} = 0.09sec. \tag{5}$$

Here, the time constant $\tau_{VVT} = 0.09sec$ is selected to capture the VVT system dynamics at an engine speed for 2000 RPM.

The throttle angle is the primary control variable in a turbocharged engine for accomplishing the torque demanded by the driver at part load and lightly boosted conditions. Here θ_{base} is defined as the base throttle signal issued in response to a driver's torque demand. Then, a compensation angle θ^{*} is introduced in addition to the base throttle signal θ_{base} in order to reduce the deleterious effects of valve overlap transitions on the cylinder charge flow rate. At a fixed or slowly varying engine speed, the compensation angle θ^{*} is selected so that the effects of the valve overlap transition

on the change rate of the cylinder charge flow rate, $\dot{W}_{cyl}$, is compensated and the associated cylinder charge flow rate, W_{cyl}, matches as much as possible the desired steady-state cylinder charge flow rate, W_{cyl}^{des}, as a result of the static valve overlap schedule v_{air} for maximum torque. From (1), we get $\dot{W}_{cyl} = \left(\frac{\partial \alpha_1}{\partial v} p_{im} + \frac{\partial \alpha_2}{\partial v}\right) + \alpha_1 \dot{p}_{im}$, hence the rate of change of cylinder air flow $\dot{W}_{cyl}(N, v_{egr}^{act})$ when the static valve overlap schedule for optimized iEGR, v_{egr}, is used is given by

$$\dot{W}_{cyl}\Big|_{v_{egr}} = \alpha_1(N, v_{egr}) K_{im} \left(g_1(\theta_{base} + \theta^*, p_b) g_2(p_{im}/p_b) - W_{cyl}\right) + \left(\frac{\partial \alpha_1}{\partial v_{egr}}\Big|_{N, v_{egr}} p_{im} + \frac{\partial \alpha_2}{\partial v_{egr}}\Big|_{N, v_{egr}}\right) \dot{v}_{egr}^{act}, \quad (6)$$

For details of static VVT schedule v_{egr} and v_{air}, please refer to Section III and Fig. 6.

It is desirable to have the $\dot{W}_{cyl}\big|_{v_{egr}}$ follow the the rate of cylinder air flow rate associated to the "best torque" static v_{air} schedule $\dot{W}_{cyl}\big|_{v_{air}}$ when the overlap schedule is performed infinitely slowly (v_{air}^{∞}) so that it does not have any impact on the transient torque responses

$$\dot{W}_{cyl}\Big|_{v_{air}^{\infty}} = \dot{W}_{cyl}^{des} = \alpha_1(N, v_{air}) K_{im} \left(g_1(\theta_{base}, p_b) g_2(\tilde{p}_{im}/p_b) - W_{cyl}^{des}\right), \quad (7)$$

where $\tilde{p}_{im}$ is a fictitious reference manifold pressure derived only with the throttle θ_{base} and engine speed N,

$$\dot{\tilde{p}}_{im} = K_{im}(g_1(\theta_{base}, p_b) g_2(\tilde{p}_{im}/p_b) - W_{cyl}). \quad (8)$$

Based on the assumption that $\frac{\partial W_{cyl}}{\partial p_{im}}\big|_{v_{egr}} \simeq \frac{\partial W_{cyl}}{\partial p_{im}}\big|_{v_{air}}$ which can be verified from Fig. 6, it follows that $\alpha_1(N, v_{egr}) \simeq \alpha_1(N, v_{air})$ and $\alpha_1(N, v_{egr}) W_{cyl}\big|_{v_{egr}} \simeq \alpha_1(N, v_{air}) W_{cyl}\big|_{v_{air}} = \alpha_1(N, v_{air}) W_{cyl}^{des}$. With these two approximations we can solve for θ^* using (6) = (7)

$$\theta^* = g_1^{-1}\left(C_1 \dot{v}_{egr}^{act} + C_2\right) - \theta_{base}, \quad (9)$$

$$\text{where} \quad C_1 = -\frac{\frac{\partial \alpha_1(N, v_{egr}^{act})}{\partial v_{egr}^{act}} p_{im} + \frac{\partial \alpha_2(N, v_{egr}^{act})}{\partial v_{egr}^{act}}}{K_{im} \alpha_1(N, v_{egr}^{act}) g_2(p_{im}/p_b)}$$

$$C_2 = \frac{g_2(\tilde{p}_{im}/p_b)}{g_2(p_{im}/p_b)} g_1(\theta_{base}, p_b).$$

The block diagram for the throttle based compensator for the VVT turbocharged engine is illustrated in Fig. 8.

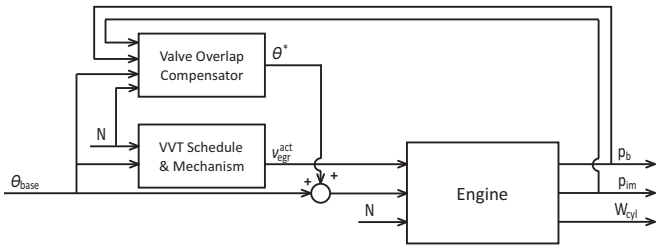

Fig. 8. Schematic diagram of VVT turbocharged engine with valve compensator.

The nonlinear engine model with the adiabatic inlet manifolds validated in Section II is used for a comparison of the cylinder air charge flow rate W_{cyl} in the VVT turbocharged engine with and without the compensation θ^* during throttle (load) step changes as shown in Fig. 9. All simulations are performed under the assumption that the fuel injectors and spark ignition are controlled perfectly such that the engine operates at stoichiometric AFR (14.6) and Maximum Brake Torque (MBT) for a given cylinder charge flow rate. Throttle step changes are introduced while the engine speed N is fixed at 2000 RPM and the static VVT schedule v_{air} is selected on at the given throttle angle and engine speed. The compensated throttle input θ^* is shown in the bottom plot of Fig. 9 as the difference between the red dash-dot line and the blue dotted line. The use of the compensated throttle angle clearly improves the transient response of W_{cyl} during throttle step change at low loads (i.e., θ_{base} = 20% $\rightarrow$ 25%) by accelerating the transition of cylinder charge flow rate to a new steady-state value. However, the load change as a result of a change of the base throttle angle from 25% to 35% does not improve significantly. During the transition of a base throttle from 35% to 45%, the compensated throttle θ^* does not improve, instead slightly deteriorates the drivability due to a small overshoot in the transient response of cylinder charge flow rate. The poor performance of the valve compensator θ^* at these conditions should be expected because there is in fact no valve overlap change to compensate for. The valve compensator θ^* is designed to address the effects of $\dot{v})egr$ and thus can not contribute much when $\dot{v})egr = 0$. Note that the difference of steady-state values of W_{cyl} between the compensated and uncompensated throttle is introduced by the difference between v_{egr} and v_{air} valve overlap schemes as discussed in Fig. 6. To achieve better cylinder charge transient response at high load and thus at high intake manifold pressure, a pressure compensator is developed in the following section to address the limitation caused by the turbo lag.

V. Pressure Compensator Design

In the previous section, a valve compensator has shown its ability to compensate the effect of valve transition on the transient response of W_{cyl} especially at low load. However, at high load, the compensator is no longer able to improve cylinder charge rate W_{cyl} transient performance as depicted in Fig. 9. The primary limitation to achieve fast response of W_{cyl} at high load is not the valve overlap change but the delayed response of boost pressure p_b, also known as Turbo Lag. Moreover, the compensation θ^* is designed to mainly cancel the effect of the overlap change using a disturbance term proportional to $\dot{v}_{egr}^{act}$ in (9) such that θ^* has little effect when the overlap change is completed, $\dot{v}_{egr}^{act}$ = 0. To extend the throttle compensator authority, a Proportional (P) feedback controller, called pressure compensator, is designed

$$\theta_{fb} = k_P \left(p_{im}^{des} - p_{im}\right), \quad (10)$$

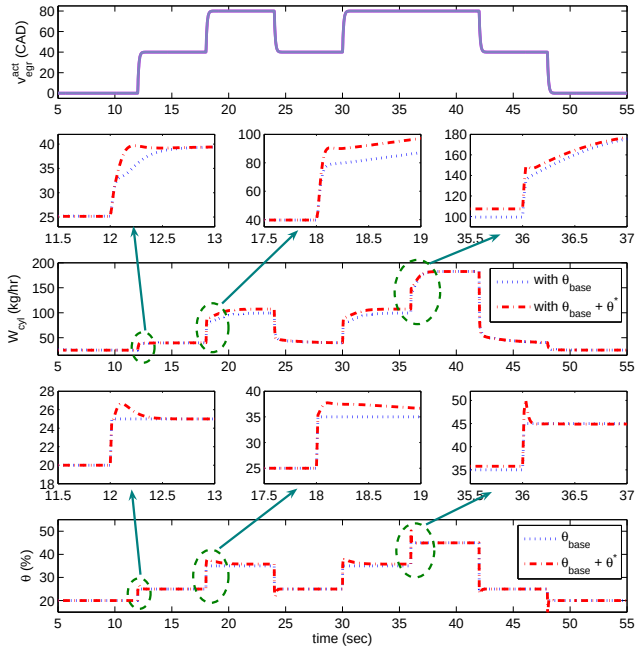

Fig. 9. Comparison of the throttle step cylinder air charge flow rate W_{cyl} of VVT turbocharged engine without compensation θ^* (blue dotted lines) and VVT turbocharged engine with compensation (red dash-dot lines); engine speed is 2000 RPM, throttle is stepped as θ_{base} = 20 → 25% → 35% → 25% → 35% → 45% → 25% → 20%.

where p_{im}^{des} is a desired intake manifold pressure at steady state, which is determined using (1)

$$p_{im}^{des} = \frac{1}{\alpha_1(N, v_{air})}\left(W_{cyl}^{des} - \alpha_2(N, v_{air})\right). \qquad (11)$$

Here, the desired cylinder air charge flow rate W_{cyl}^{des} can be simply extracted from the first plot in Fig. 6. For better implementation, a low pass filter with a time constant of 0.06 sec is used for p_{im}^{des}. The corresponding block diagram of the engine with the valve compensator for the valve overlap adjustment and the pressure compensator for the desired pressure adjustment is shown in Fig. 10.

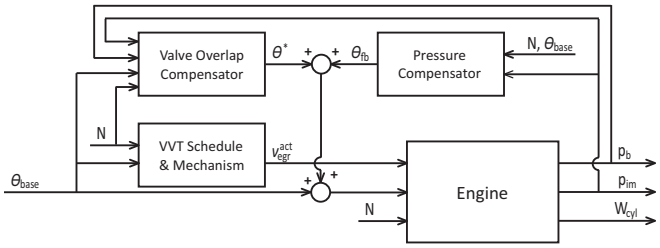

Fig. 10. Schematic diagram of VVT turbocharged engine with valve compensator and pressure compensator.

The cylinder charge flow rate W_{cyl} response for the valve compensated and the pressure compensated throttle signal is shown in Fig. 11. The pressure compensation controller enhances the W_{cyl} transient behavior for each throttle step changes. It can be observed that the combined use of the valve and pressure compensators can eliminate small overshoot during the transition of θ = 20% → 25%, and achieve faster and smoother transition to steady state at both θ = 25% → 35% and θ = 35% → 45% transients. Compared to the valve compensation, the pressure compensation keeps the throttle open for a longer time with bigger peak values until the intake manifold pressure reaches the steady state condition. A better understanding of the compensated system response can be obtained by investigating the boost pressure p_b and intake manifold pressure p_{im} responses during step changes shown in Fig. 12. Note that the pressure compensator in addition to the valve compensator also achieves better transient behavior of W_{cyl} during tip-outs. The pressure compensator alone, however, does not achieve a comparable W_{cyl} transient behavior, which clearly indicates the necessity of both compensators.

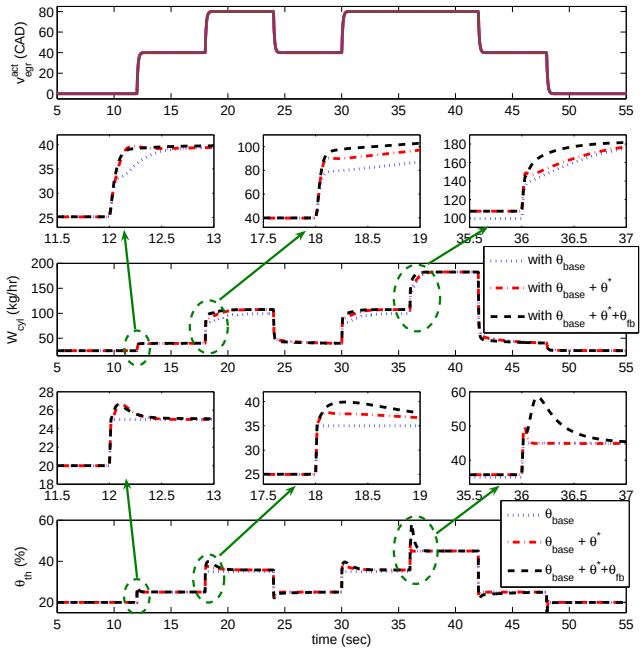

Fig. 11. Comparison of the throttle step cylinder air charge flow rate W_{cyl} of VVT turbocharged engine without compensation θ^* (blue dotted lines), VVT turbocharged engine with compensation (red dash-dot lines) and VVT turbocharged engine with compensation plus Proportional controller (blue dashed lines); engine speed is 2000 RPM, throttle is stepped as θ_{base} = 20 → 25% → 35% → 25% → 35% → 45% → 25% → 20%.

Intake manifold pressure p_{im} drives the cylinder charge flow rate W_{cyl} after the valve overlap transition is completed. The pressure compensator generates a longer and wider throttle opening during tip-ins such that the intake manifold pressure p_{im} approaches the boost pressure p_b at a faster rate compared to the cases only with the valve compensation. Therefore, the fast transient behavior of p_{im} using the aggressive throttle opening can be only achieved when the boost pressure is relatively higher than the intake manifold pressure at the moment when the throttle step is applied.

VI. Conclusions and Future Works

This paper presents a modification of the nonlinear mean value model [6] of a turbocharged spark ignition flex-

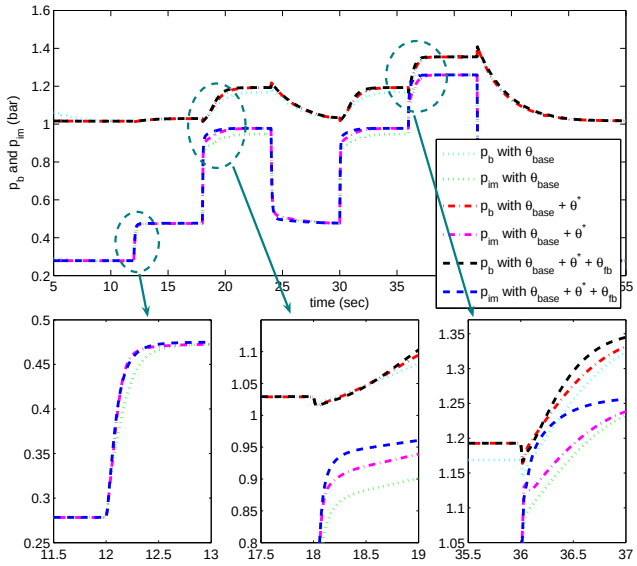

Fig. 12. Comparison of the boost pressure p_b and intake manifold pressure p_{im} of VVT turbocharged engine without compensation, with throttle based compensation, and with throttle based compensation plus Proportional feedback controller.

fuel engine equipped with variable camshafts and electronic throttle. Two static valve overlap schedules were derived for "best torque" and "best iEGR" requirements. To improve the transient behaviors of the cylinder charge air flow rate (or torque) during throttle step changes, the valve compensator and the pressure compensator have been introduced in the air-path control loop. To reduce the disturbance of the VVT change on cylinder charge flow rate, a nonlinear model-based valve compensator was designed in addition to the base throttle controller for the turbocharged engine. This compensator improves the transient behavior of cylinder charge flow rate, especially at low load. Due to the limited capability of the compensator to achieve fast response of cylinder flow rate at high load, a pressure compensation was included for transient performance enhancement. The valve compensator and pressure compensator together showed a considerable improvement with a more aggressive throttle opening strategy resulting in longer and wider throttle openings compared to the throttle compensator alone.

In future work, we will focus on wastegate actuator to address the boosted engine behavior. The wastegate and associated exhaust flow dynamics can lead to more complex interactions with throttle and VVT transitions. The additional actuator of wastegate can lead to more complicated engine system and careful system analysis, therefore, is required. New control structure needs to be designed based on the engine system analysis. In addition, engine rotational dynamics should be considered to eliminate the fixed engine speed assumption for more realistic application. Finally, we will implement the proposed control structure on a vehicle and evaluate its robustness properties.

REFERENCES

[1] A. G. Stefanopoulou and I. Kolmanovsky, "Analysis and control of transient torque response in engines with internal exhaust gas recirculation," *IEEE Transactions on Control Systems Technology*, vol. 7, no. 5, pp. 555 – 566, 1999, internal exhaust gas recirculation;. [Online]. Available: http://dx.doi.org/10.1109/87.784419

[2] M. Jankovic, F. Frischmuth, A. Stefanopoulou, and J. A. Cook, "Torque management of engines with variable cam timing," *IEEE Control Systems Magazine*, vol. 18, no. 5, pp. 34 – 42, 1998. [Online]. Available: http://dx.doi.org/10.1109/37.722251

[3] M. Muller, E. Hendricks, and S. C. Sorenson, "Mean value modelling of turbocharged spark ignition engines," in *SAE Special Publications*, vol. 1330, Detroit, MI, USA, 1998, pp. 125 – 145.

[4] L. Eriksson, L. Nielsen, J. Brugard, J. Bergstrom, F. Pettersson, and P. Andersson, "Modeling of a turbocharged si engine," *Annual Reviews in Control*, vol. 26 I, pp. 129 – 137, 2002. [Online]. Available: http://dx.doi.org/10.1016/S1367-5788(02)80022-0

[5] A. Y. Karnik, J. H. Buckland, and J. S. Freudenberg, "Electronic throttle and wastegate control for turbocharged gasoline engines," in *Proceedings of the American Control Conference*, vol. 7, Portland, OR, United states, 2005, pp. 4434 – 4439.

[6] L. Jiang, A. Stefanopoulou, J. Vanier, and H. Yilmaz, "Parameterization and simulation for a turbocharged spark ignition direct injection engine with variable valve timing," in *SAE Technical Paper*, no. 2009-01-0680, Detroit, MI, United States, 2009.

[7] R. J. Wakeman and D. O. Wright, "Closed loop turbocharger control with transient wastegate functions," in *SAE Special Publications*, Detroit, MI, Untied States, 1986, pp. 131 – 135.

[8] J. R. Zurlo, E. O. Reinbold, and J. Mueller, "Waukesha turbocharger control module: a tool for improved engine efficiency and response," in *American Society of Mechanical Engineers, Internal Combustion Engine Division (Publication) ICE*, vol. 27-4, Fairborn, OH, USA, 1996, pp. 35 – 40.

[9] J. Buckland, J. Grizzle, J. Freudenberg, and J. J., "Estimation of exhaust manifold pressure in turbocharged gasoline engines with variable valve timing," in *Proceedings of the ASME 2008 Dynamics Systems and Control Conference*, Ann Arbor, MI USA, 2008.

[10] J. H. Buckland, J. S. Freudenberg, G. J. W., and M. Jankovic, "Practical observers for unmeasured states in turbocharged gasoline engines," in *American Control Conference*, Seattle, MO, United States, June 2009, pp. 2714–2719.